Toxicology Letters 225 (2014) 445–453

Contents lists available at ScienceDirect

Toxicology Letters

journal homepage: www.elsevier.com/locate/toxlet

Role of receptor interacting protein (RIP)1 on apoptosis-inducing factor-mediated necroptosis during acetaminophen-evoked acute liver failure in mice

Ye-Fa Zhang[a,1], Wei He[b,1], Cheng Zhang[a,1], Xiao-Jing Liu[b], Yan Lu[c], Hua Wang[a], Zhi-Hui Zhang[a], Xi Chen[b,**], De-Xiang Xu[a,*]

[a] Department of Toxicology, Anhui Medical University, Hefei 230032, China
[b] First Affiliated Hospital, Anhui Medical University, Hefei 230022, China
[c] Second Affiliated Hospital, Anhui Medical University, Hefei 230601, China

HIGHLIGHTS

- RIP1 is an early mediator of APAP-induced hepatocyte death.
- Nec-1 improved the survival and prevented from APAP-induced hepatocyte death.
- Nec-1 obviously inhibited APAP-induced hepatic JNK activation.
- Nec-1 attenuates APAP-induced mitochondrial Bax and nuclear AIF translocation.
- Nec-1 is an effective antidote for APAP-induced acute liver failure.

ARTICLE INFO

Article history:
Received 15 October 2013
Received in revised form
24 December 2013
Accepted 1 January 2014
Available online 17 January 2014

Keywords:
Acetaminophen
Necroptosis
Receptor-interacting protein (RIP) kinases
Apoptosis-inducing factor (AIF)
Necrostatin-1 (Nec-1)

ABSTRACT

Acetaminophen (APAP) overdose induces apoptosis-inducing factor (AIF)-dependent necroptosis, but the mechanism remains obscure. The present study investigated the role of receptor interacting protein (RIP)1, a critical mediator of necroptosis, on AIF-dependent necroptosis during APAP-induced acute liver failure. Mice were intraperitoneally injected with APAP (300 mg/kg). As expected, hepatic RIP1 was activated as early as 1 h after APAP, which is earlier than APAP-induced hepatic RIP3 upregulation. APAP-evoked RIP1 activation is associated with hepatic glutathione (GSH) depletion. Either pretreatment or post-treatment with Nec-1, a selective inhibitor of RIP1, significantly alleviated APAP-induced acute liver failure. Moreover, Nec-1 improved the survival and prevented APAP-induced necroptosis, as determined by TdT-mediated dUTP-biotin nick end labeling (TUNEL) assay. Further analysis showed that Nec-1 significantly inhibited APAP-induced hepatic c-Jun N-terminal kinase (JNK) phosphorylation and mitochondrial Bax translocation. In addition, Nec-1 blocked APAP-induced translocation of AIF from the mitochondria to the nucleus. Of interest, no changes were induced by Nec-1 on hepatic CYP2E1 expression. In addition, Nec-1 had little effect on APAP-induced hepatic GSH depletion at early stage. Taken together, these results suggest that RIP1 is involved in APAP-induced necroptosis. Nec-1 is an effective antidote for APAP-induced acute liver failure.

1. Introduction

Acetaminophen (APAP) is a widely used analgesic and antipyretic drug. Although safe at therapeutic doses, APAP overdose can cause severe acute liver failure (Jaeschke and Bajt, 2006). APAP-induced liver injury is initiated by the formation of a reactive metabolite, *N*-acetyl-*p*-benzoquinone imine (NAPQI), which can be generated by several cytochrome P450 (CYP) isoenzymes, especially CYP2E1 (Zaher et al., 1998). According to several reports, the prolonged activation of c-Jun *N*-terminal kinase (JNK) plays

* Corresponding author at: Department of Toxicology, Anhui Medical University, Hefei 230032, China. Tel.: +86 551 65167923.
** Corresponding author at: Department of Gastroenterology, First Affiliated Hospital, Anhui Medical University, Hefei 230022, China.
E-mail address: xudex@126.com (D.-X. Xu).
[1] These authors contributed equally to this work.

0378-4274/$ – see front matter © 2014 Elsevier Ireland Ltd. All rights reserved.
http://dx.doi.org/10.1016/j.toxlet.2014.01.005

a key role in APAP-evoked hepatocyte death (Ghosh et al., 2010; Gunawan et al., 2006; Latchoumycandane et al., 2007). Moreover, apoptosis-inducing factor (AIF), which translocates to the nucleus and initiates nuclear DNA fragmentation, may be a critical mediator of hepatocyte death during APAP-induced acute liver failure (Bajt et al., 2006, 2011; Ramachandran et al., 2011).

There are at least three major kinds of cell death: apoptosis, autophagy and necrosis (Galluzzi et al., 2012). Apoptosis and autophagy are a highly regulated process involving complex signaling networks (Carmona-Gutierrez et al., 2010; Kumar, 2007; Orrenius et al., 2011; Shen and Codogno, 2011). By contrast, necrosis is considered a passive, unregulated form of cell death, morphologically characterized by rounding of the cell, a gain in cell volume, organelle swelling, lack of internucleosomal DNA fragmentation, and plasma membrane rupture (Galluzzi et al., 2007). Increasing evidence demonstrates that some necrosis is evoked by regulated signal transduction pathways such as those mediated by receptor interacting protein (RIP) kinases when caspase cascade cannot be activated efficiently (Hitomi et al., 2008; Vandenabeele et al.,2010; Vanlangenakker et al., 2012). The regulated necrosis and in particular RIP1/RIP3-mediated necrosis, referred to as programmed necrosis or necroptosis, has been becoming an intensively studied form of programmed cell death (Kaiser et al., 2011; Osborn et al., 2010; Trichonas et al., 2010). According to a recent report, RIP3 is a critical mediator of necroptosis during APAP-induced acute liver failure (Ramachandran et al., 2013). Nevertheless, the role of RIP1 in the process of APAP-induced acute liver failure remains obscure.

In the present study, we hypothesize that RIP1 is involved in AIF-dependent necroptosis during APAP-induced acute liver failure. To test this hypothesis, we investigated the effects of necrostatin-1 (Nec-1), a potent and selective inhibitor of RIP1 kinase activity (Degterev et al., 2008; Xie et al., 2013), on APAP-induced necroptosis. We show that pretreatment or post-treatment with Nec-1 alleviated APAP-induced acute liver failure. Moreover, Nec-1 improved the survival and prevented APAP-induced necroptosis. In addition, Nec-1 inhibits APAP-induced hepatic JNK phosphorylation and mitochondrial Bax translocation. We demonstrated that RIP1 is involved in AIF-dependent necroptosis during APAP-induced acute liver failure. Nec-1 is an effective antidote for APAP-induced acute liver failure.

2. Materials and methods

2.1. Chemicals and reagents

Acetaminophen (APAP), *N*-acetylcysteine (NAC) and buthionine sulfoximine (BSO) were purchased from Sigma Chemical Co. (St. Louis, MO). Necrostatin-1 (Nec-1) was purchased from Santa Cruz Biotechnology Inc (Santa Cruz, CA). All other reagents were purchased from Sigma Chemical Co. (St. Louis, MO) if not otherwise stated.

2.2. Animals and treatments

Male CD-1 mice (6–8 week-old, 28–30 g) were purchased from Beijing Vital River (Beijing, China). The animals were allowed free access to food and water at all times and were maintained on a 12-h light/dark cycle in a controlled temperature (20–25 °C) and humidity (50 ± 5%) environment for a period of 1 week before use. After a 12-h fast, mice were intraperitoneally (i.p.) injected with APAP (300 mg/kg). For Nec-1 pretreatment, mice were i.p. injected with Nec-1 (0.125 mg/mouse) 30 min before APAP. For Nec-1 post-treatment, mice were i.p. injected with Nec-1 (0.125 mg/mouse) 30 min after APAP. Serum and liver samples were collected at 4 h or 24 h after APAP. To investigate the effects of Nec-1 on hepatic APAP metabolism, mice were i.p. injected with Nec-1 (0.125 mg/mouse) 30 min before APAP and liver samples were collected at 30 min after APAP. To investigate whether Nec-1 protects against APAP-induced hepatocyte death through its antioxidant activity, mice were i.p. injected with APAP (300 mg/kg). In BSO + Nec-1 + APAP groups, mice were administered with BSO before Nec-1. Serum and liver samples were collected 4 h after APAP. The doses of Nec-1 used in the present study referred to others (Duprez et al., 2011). This study was approved by the Association of Laboratory Animal Sciences and the Center for Laboratory Animal Sciences at Anhui Medical University (Permit number: 12-0010). All procedures on animals followed the Guide for the Care and Use of Laboratory Animals published by the US National Institutes of Health (NIH Publication no. 85-23, revised 1996).

2.3. Evaluation of liver injury

Serum alanine aminotransferase (ALT) were measured using commercially available assay kits according to the manufacturer's instructions. Liver tissues were fixed in 4% formalin and embedded in paraffin according to the standard procedure. Paraffin embedded tissues were cut 5 mm thick and stained with hematoxylin and eosin (H & E) for morphological analysis. To quantify the extent of necrosis, the percentage of necrosis was estimated by measuring the necrotic area relative to the entire histological section, and an analysis of the area was performed with NIH ImageJ software (http://rsb.info.nih.gov/ij/).

2.4. Measurement of hepatic GSH content

Hepatic GSH and GSSG contents were determined by the DTNB–GSSG reductase recycling assay as described by Anderson (1985), with some modifications. GSH was expressed as μmol/g liver.

2.5. Immunoblots

Immunoblots were performed using liver lysates and subcellular fractions. In brief, protein extracts from each sample were separated electrophoretically by SDS-PAGE and transferred to a polyvinylidene fluoride membrane. For mitochondrial protein, the membranes were incubated for 2 h with following antibodies: Bax, RIP1, RIP3, JNK and pJNK. For total proteins, the membranes were incubated for 2 h with following antibodies: RIP1, RIP3, pJNK, CYP2E1 and 3-NT. For total proteins, α-tubulin was used as a loading control. For mitochondrial protein, Porin was used as a loading control. After washes in DPBS containing 0.05% Tween-20 four times for 10 min each, the membranes were incubated with goat anti-rabbit or goad anti-mouse IgG antibodies for 2 h. The membranes were washed for four times in DPBS containing 0.05% Tween-20 for 10 min each, followed by signal development using an ECL detection kit.

2.6. Isolation of total RNA and real-time RT-PCR

Total RNA was extracted using TRI reagent. The purity of RNA was assessed according to the ratio of absorbance at 260 nm and 280 nm. RNase-free DNase-treated total RNA (1.0 μg) was reverse-transcribed with AMV. Real-time RT-PCR was performed with a GoTaq® qPCR master mix using gene-specific primers as follow. *Tnf-α*, CCC TCC TGG CCA ACG GCA TG, TCG GG GCA GCC TTG TCC CTT; *Gapdh*, ACC CCA GCA AGG ACA CTG AGC AAG, GGC CCC TCC TGT TAT TAT GGG GGT. The amplification reactions were carried out on a LightCycler® 480 Instrument (Roche Diagnostics GmbH, Mannheim, Germany) with an initial hold step (95 °C for 5 min) and 50 cycles of a three-step PCR (95 °C for 15 s, 60 °C for 15 s, 72 °C for 30 s). The comparative C_T-method (Hoebeeck et al., 2007; Ferlini and Rimessi, 2012) was used to determine the amount of target, normalized to an endogenous reference and relative to a calibrator ($2^{-\Delta\Delta Ct}$) using the Lightcycler 480 software (Roche, version 1.5.0). All RT-PCR experiments were performed in triplicate.

2.7. Immunohistochemistry

Paraffin-embedded sections were deparaffinized and rehydrated in a graded ethanol series. After antigen retrieval and quenching of endogenous peroxidase, sections were incubated with AIF monoclonal antibodies (1:200 dilution) at 4 °C overnight. The color reaction was developed with HRP-linked polymer detection system and counterstaining with hematoxylin.

2.8. Terminal dUTP nick-end labeling (TUNEL) staining

For the detection of nuclear DNA strand breaks, paraffin-embedded sections were stained with the TUNEL technique using an in situ apoptosis detection kit (Promega Madison, WI) according to the manufacturer's protocols. Sections were counterstained with hematoxylin. TUNEL-positive cells were counted in twelve randomly selected fields from each slide at a magnification of ×200. The percentage of TUNEL-positive hepatocytes was analyzed in six liver sections from six different mice.

2.9. Statistical analysis

All quantified data were expressed as means ± SE at each point. ANOVA and the Student–Newmann–Keuls post hoc test were used to determine differences among different groups.

3. Results

3.1. APAP upregulates hepatic RIP1 and RIP3

The effects of APAP on the expression of hepatic RIP1 and RIP3 were analyzed. As shown in Fig. 1A, the expression of hepatic RIP1 was significantly increased as early as 1 h after APAP. Correspondingly, hepatic RIP3 was significantly upregulated in a time-dependent manner (Fig. 1B). To investigate whether RIP3 is a downstream molecule of RIP1, the effects of Nec-1 on the expression of hepatic RIP3 was analyzed. As expected, Nec-1 significantly attenuated APAP-induced upregulation of hepatic RIP3 (Fig. 1C). The effects of APAP on hepatic GSH content are shown in Fig. 1D. As expected, GSH content was significantly decreased as early as 1 h after APAP. To investigate the role of hepatic GSH depletion on APAP-induced upregulation of hepatic RIP1 and RIP3, the effects of NAC, a well-known GSH precursor, on APAP-induced hepatic RIP1 and RIP3 expression were then analyzed. As shown in Fig. 1E, pretreatment with NAC significantly attenuated APAP-induced upregulation of hepatic RIP1. In addition, pretreatment with NAC significantly attenuated APAP-induced upregulation of hepatic RIP3 (Fig. 1F). The effects of APAP on the expression of hepatic TNF-α were analyzed. As shown in Fig. 1G, no significant difference on hepatic TNF-α mRNA was observed between APAP-treated mice and controls.

3.2. Pretreatment with Nec-1 protects against APAP-induced hepatocyte death

As shown in Fig. 2A, serum ALT was significantly elevated 4 h after APAP. Histopathology showed an obvious congestion in liver of APAP-treated mice (Fig. 2B). A characteristic centrilobular necrosis was observed in liver section of mice administered with APAP. Necrotic area was about 36% 4 h after APAP (Fig. 2C). Serum ALT remained increased 24 h after APAP (Fig. 2D). The characteristic centrilobular necrosis remained observed 24 h after APAP (Fig. 2E). The area of necrosis was above 40% at 24 h after APAP (Fig. 2F). Additional experiment showed that 70% mice (7/10) were dead in 72 h after APAP (Fig. 2G). The effects of pretreatment with Nec-1, a specific RIP1 inhibitor, on APAP-induced acute liver injury were analyzed. Of interest, pretreatment with Nec-1 improved the survival (Fig. 2G) and alleviated APAP-induced increase in serum ALT (Fig. 2A and D). Correspondingly, pretreatment with Nec-1 completely prevented from APAP-induced centrilobular necrosis (Fig. 2B, C, E and F). APAP-induced hepatocyte death was determined by TUNEL assay. As shown in Fig. 2H, numerous TUNEL+ hepatocytes were observed in liver of APAP-treated mice. Of interest, pretreatment with Nec-1 significantly attenuated APAP-induced elevation of TUNEL+ hepatocytes (Fig. 2I).

3.3. Effects of Nec-1 on hepatic APAP metabolism

To investigate whether Nec-1 by itself can alter APAP metabolism, the effects of Nec-1 pretreatment on hepatic GSH depletion were analyzed at 30 min after APAP. As expected, hepatic GSH was significantly decreased 30 min after APAP. Of interest, pretreatment with Nec-1 did not affect the level of hepatic GSH at 30 min after APAP (Fig. 3A). The effects of Nec-1 pretreatment on hepatic CYP2E1, a main metabolic enzyme of APAP, were then analyzed. As shown in Fig. 3B, pretreatment with Nec-1 had no effect on the expression of hepatic CYP2E1.

3.4. Nec-1 attenuates APAP-induced JNK phosphorylation

As expected, APAP significantly increased the level of hepatic phosphorylated JNK in a time-dependent manner (Fig. 4A).

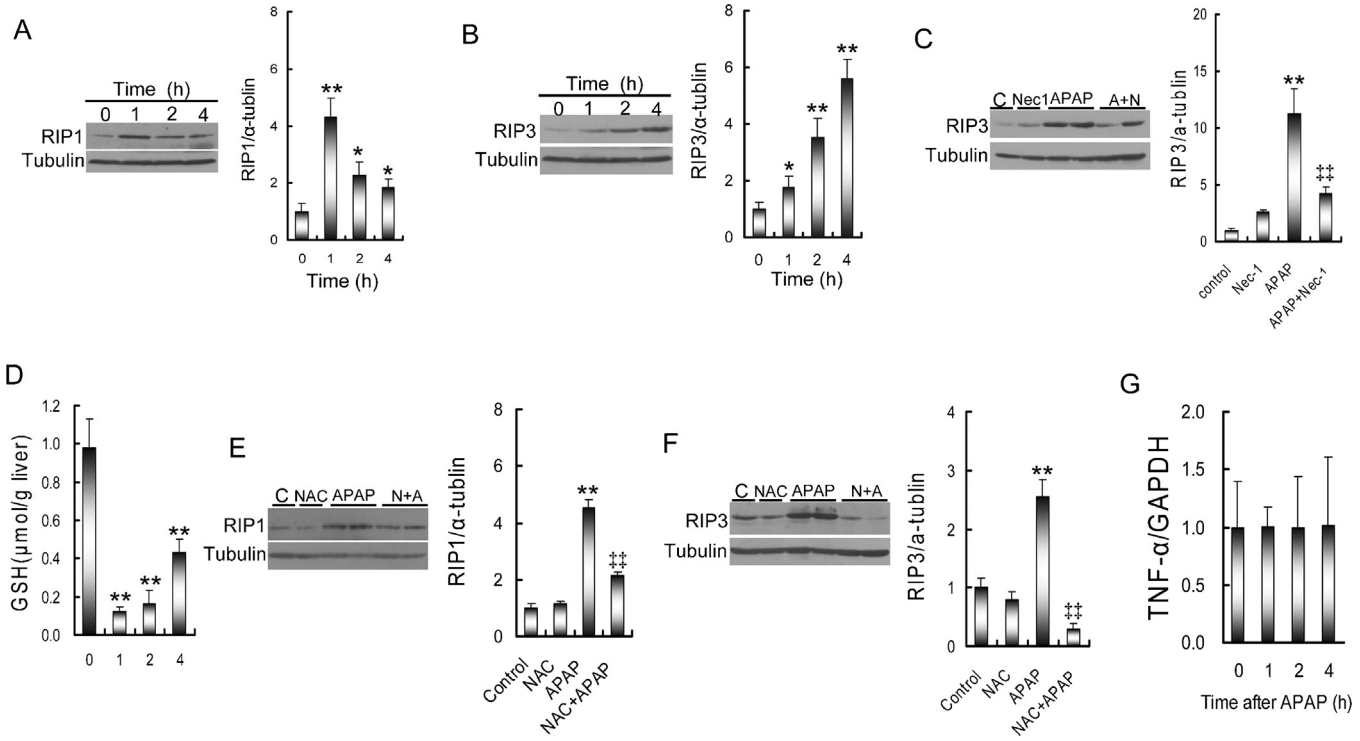

Fig. 1. GSH depletion mediates APAP-evoked upregulation of hepatic RIP1 and RIP3. (A and B) Mice were i.p. injected with APAP (300 mg/kg). Hepatic (A) RIP1 and (B) RIP3 were determined by immunoblots. (C) Mice were i.p. injected with Nec-1 (0.125 mg/mouse) 30 min before APAP. Hepatic RIP3 was determined by immunoblots. (D) Mice were i.p. injected with APAP (300 mg/kg). Hepatic GSH content was measured. (E and F) Mice were i.p. injected with NAC (1500 mg/kg) before APAP (300 mg/kg). Liver samples were collected 4 h after APAP. Hepatic (E) RIP1 and (F) RIP3 were determined by immunoblots. (G) Mice were i.p. injected with APAP (300 mg/kg). Hepatic TNF-α was detected using real-time RT-PCR. All data were expressed as means ± SEM (n = 3–6). $P < 0.05$, ** $P < 0.01$ as compared with control group.

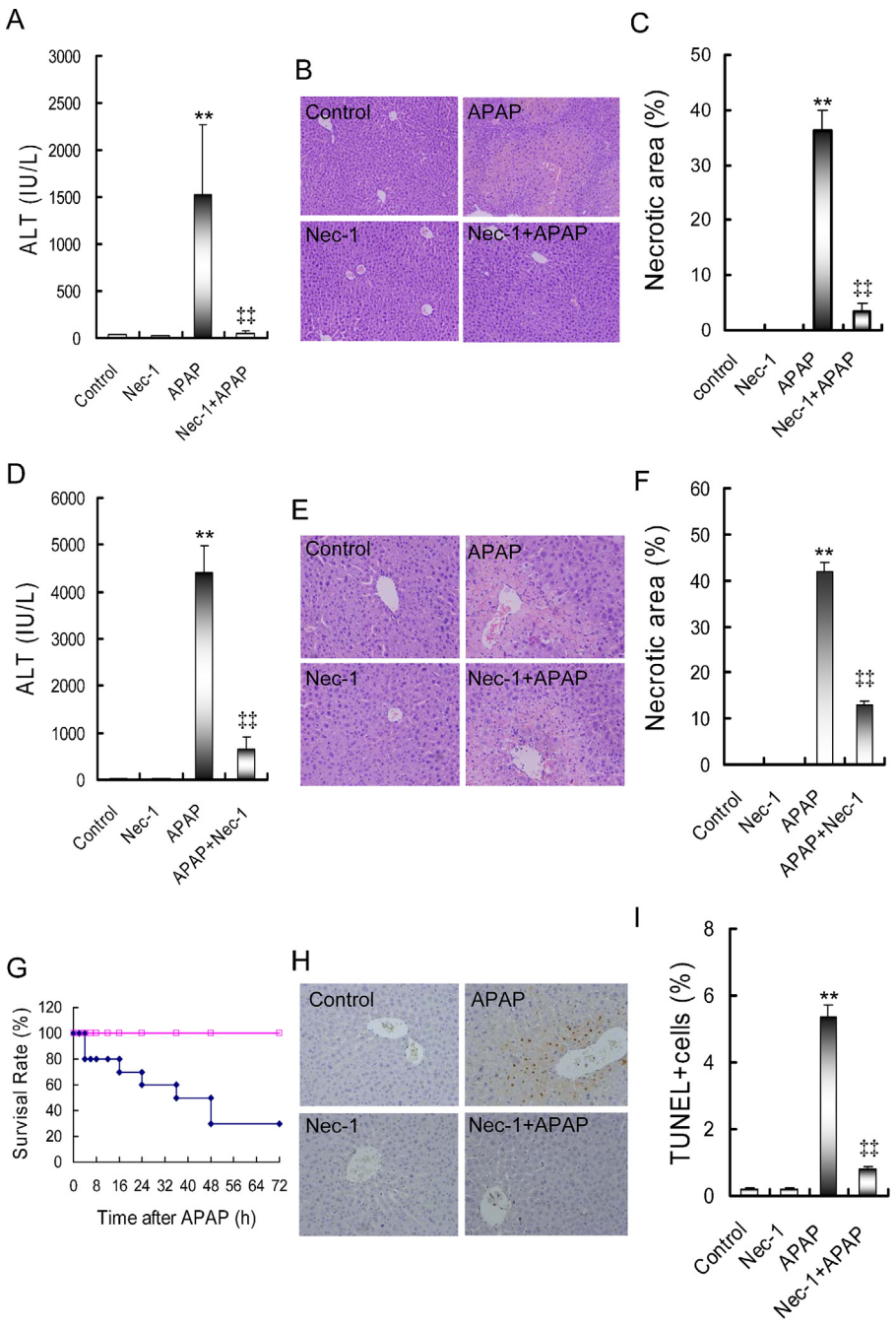

Fig. 2. Pretreatment with Nec-1 protects against APAP-induced liver injury. Mice were i.p. injected with APAP (300 mg/kg). In APAP + Nec-1 group, mice were i.p. injected with Nec-1 (0.125 mg/mouse) 30 min before APAP. (A–C) Serum and liver samples were collected 4 h after APAP. (A) Serum ALT. (B) Representative photomicrographs of liver histology (H & E, magnification: 100×). (C) The percentage of necrotic area was analyzed. (D–F) Serum and liver samples were collected 24 h after APAP. (D) Serum ALT. (E) Representative photomicrographs of liver histology (H & E, magnification: 100×). (F) The percentage of necrotic area was analyzed. (G) Twenty mice were divided into two groups. All mice were i.p. injected with (300 mg/kg). In APAP + Nec-1 group, mice were i.p. injected with Nec-1 (0.125 mg/mouse) 30 min before APAP. Animal death was observed until 72 h after APAP. (H) Mice were i.p. injected with APAP (300 mg/kg). Liver samples were collected 4 h after APAP. Hepatocyte death was determined using TUNEL assay. Representative photomicrographs from different groups. (I) TUNEL+ hepatocytes were analyzed. All data were expressed as means ± SEM ($n = 6$). ** $P < 0.01$ as compared with the control. ‡‡ $P < 0.01$ as compared with APAP group.

Interestingly, the level of mitochondrial phosphorylated JNK was significantly increased at 4 h after APAP (Fig. 4B). The effects of Nec-1 on APAP-induced hepatic JNK phosphorylation were analyzed. As shown in Fig. 4C, pretreatment with Nec-1 significantly attenuated APAP-evoked hepatic JNK phosphorylation. Further analysis showed that pretreatment with Nec-1 significantly attenuated APAP-induced elevation of phosphorylated JNK in the mitochondria (Fig. 4D).

3.5. *Nec-1 attenuates APAP-induced mitochondrial Bax translocation*

The effects of Nec-1 on APAP-induced translocation of Bax are presented in Fig. 4E. As expected, mitochondrial Bax level was significantly increased in liver of mice administered with APAP. Interestingly, pretreatment with Nec-1 significantly attenuated APAP-induced translocation of Bax from the cytosol to the mitochondria.

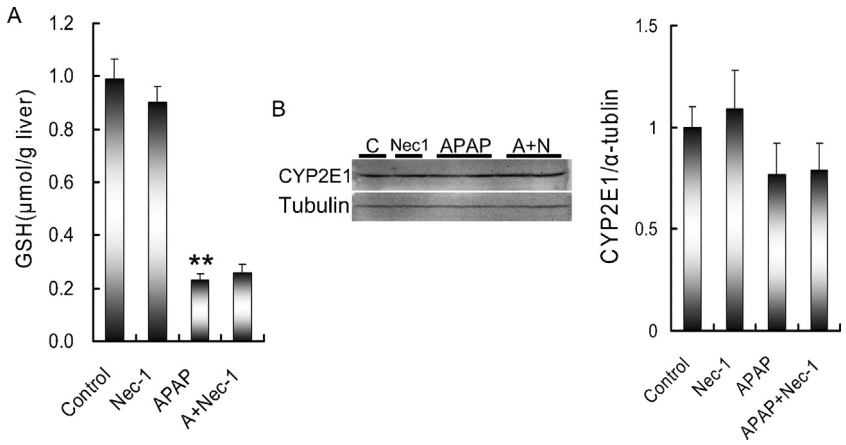

Fig. 3. Effects of Nec-1 on hepatic APAP metabolism. Mice were i.p. injected with APAP (300 mg/kg). In APAP + Nec-1 group, mice were i.p. injected with Nec-1 (0.125 mg/mouse) 30 min before APAP. Liver samples were collected 30 min after APAP. (A) Hepatic GSH content. (B) Hepatic CYP2E1 was detected using immunoblots. All data were expressed as means ± SEM ($n = 6$). ** $P < 0.01$ as compared with control group.

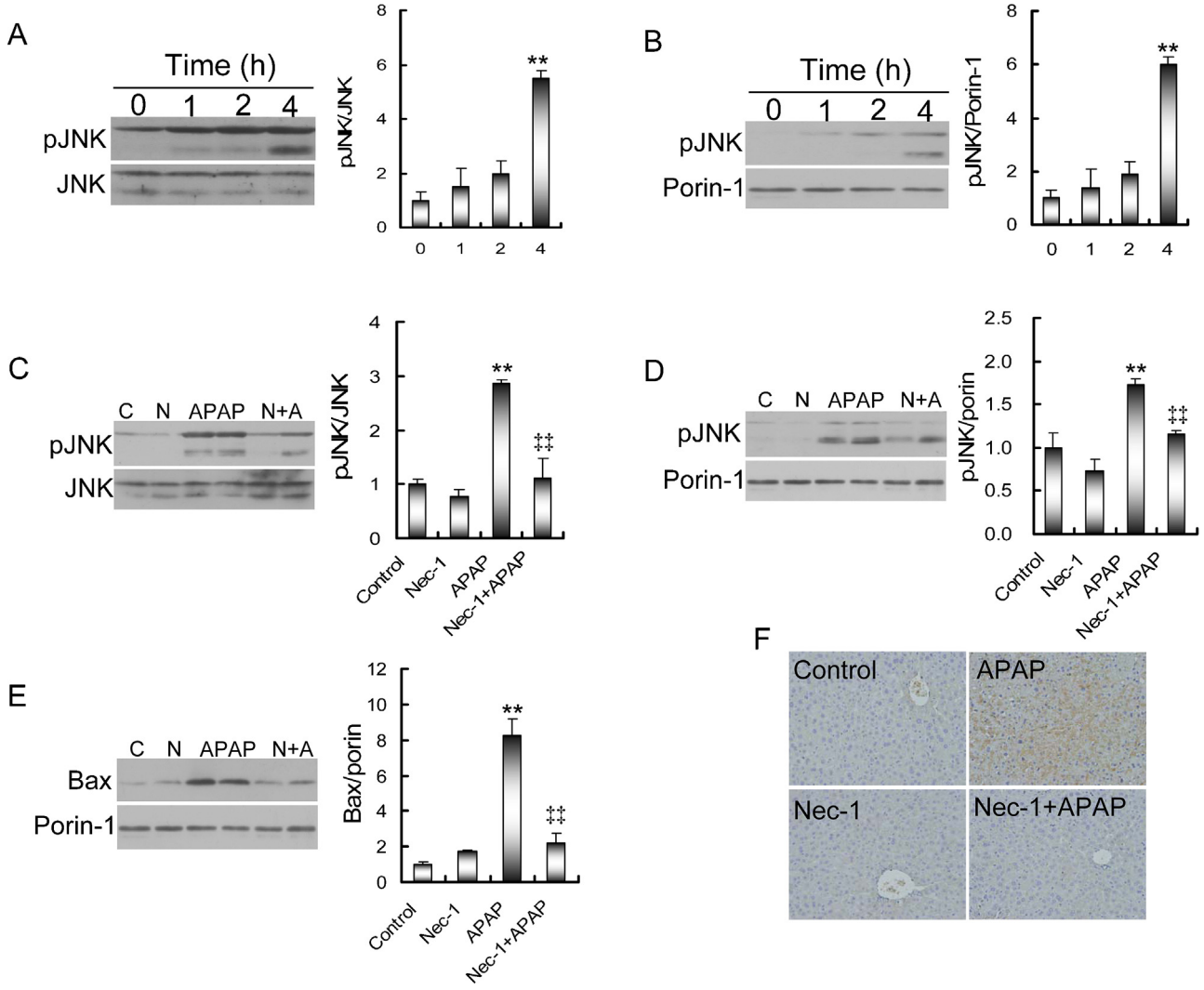

Fig. 4. Nec-1 attenuates APAP-induced hepatic JNK phosphorylation, mitochondrial Bax translocation and nuclear AIF translocation. (A and B) Mice were i.p. injected with APAP (300 mg/kg). Liver samples were collected at different time point after APAP. (A) Hepatic and (B) mitochondrial JNK phosphorylation was detected by immunoblots. (C–F) Mice were injected i.p. with Nec-1 (0.125 mg/mouse) 30 min before APAP (300 mg/kg). Liver samples were collected 4 h after APAP. (C) Hepatic and (D) mitochondrial JNK phosphorylation was detected by immunoblots. (E) Mitochondrial Bax was detected by immunoblots. (F) Nuclear AIF translocation was determined by immunohistochemistry. All data were expressed as means ± SEM ($n = 3$–6). ** $P < 0.01$ as compared with control group. ‡‡ $P < 0.01$ as compared with APAP group.

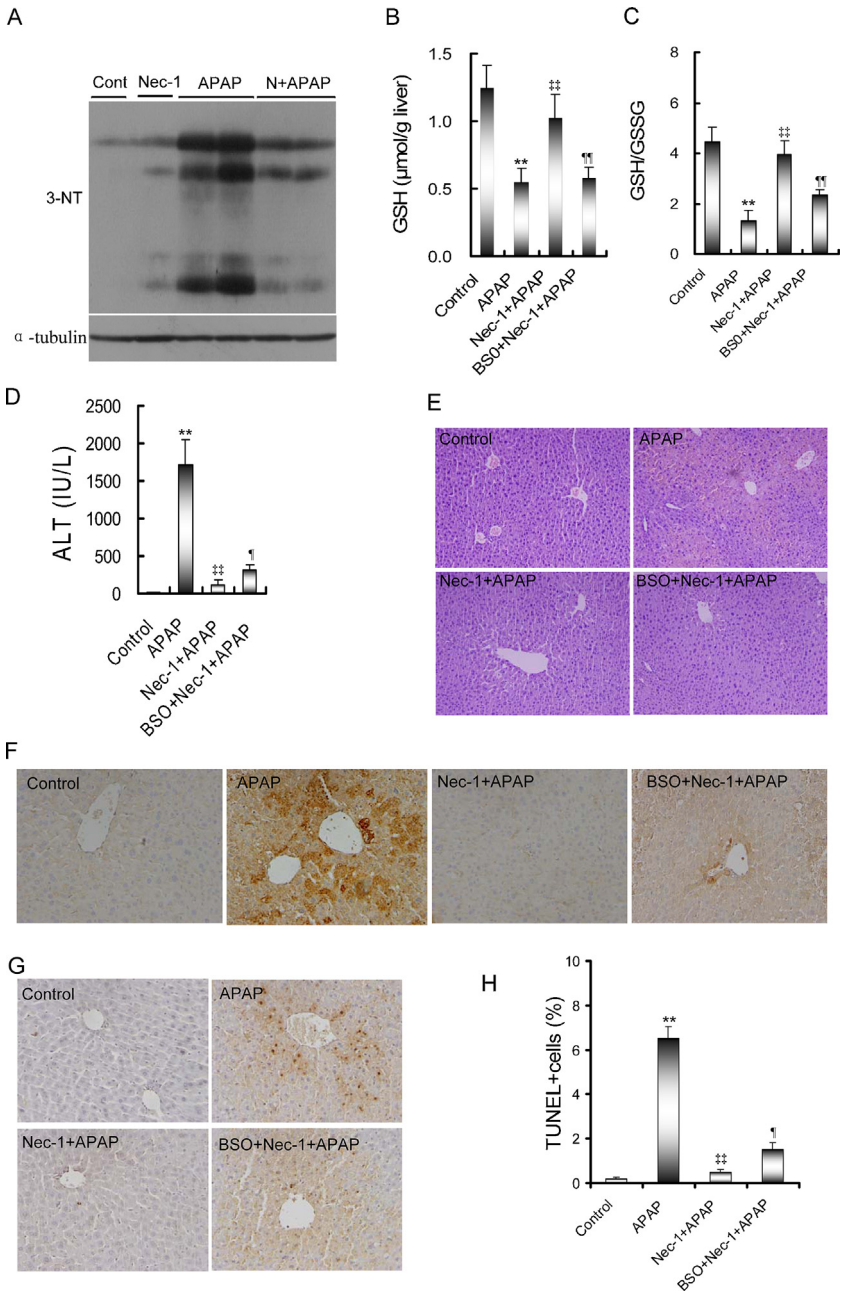

Fig. 5. Nec-1 protects mice from APAP-induced hepatocyte death independent of its antioxidant activity. (A) Mice were injected i.p. with Nec-1 (0.125 mg/mouse) 30 min before APAP (300 mg/kg, i.p.). Liver samples were collected 4 h after APAP. 3-NT was detected by immunoblots. (B–G) Mice were treated as Materials and Methods. Liver samples were collected at 4 h after APAP. (B) Hepatic GSH. (C) GSH/GSSG ratio. (D) Serum ALT. (E) Representative photomicrographs of liver histology (H & E, magnification: 100×). (F) Nuclear AIF translocation was determined by immunohistochemistry. (G) Hepatocyte death was determined using TUNEL assay. Representative photomicrographs from different groups. (H) TUNEL+ hepatocytes were analyzed. All data were expressed as means ± SEM ($n = 6$). ** $P < 0.01$ as compared with the control. ‡‡ $P < 0.01$ as compared with APAP group.

3.6. Nec-1 attenuates APAP-induced nuclear AIF translocation

The effects of Nec-1 on APAP-induced nuclear translocation of AIF were then analyzed. Immunohistochemistry showed that nuclear AIF translocation was mainly distributed around hepatic sinus (Fig. 4F). Interestingly, APAP-induced nuclear AIF translocation was almost completely inhibited when mice were pretreated with Nec-1 (Fig. 4F).

3.7. Nec-1's protective mechanism on APAP-induced hepatotoxicity is not mediated by a GSH-dependent pathway

As shown in Fig. 5A, pretreatment with Nec-1 significantly attenuated APAP-induced elevation of hepatic 3-NT, a marker of protein nitrification. In addition, pretreatment with Nec-1 significantly attenuated APAP-induced hepatic GSH depletion (Fig. 5B and C). γ-glutamylcysteine synthetase (γ-GCS) is a critical enzyme in

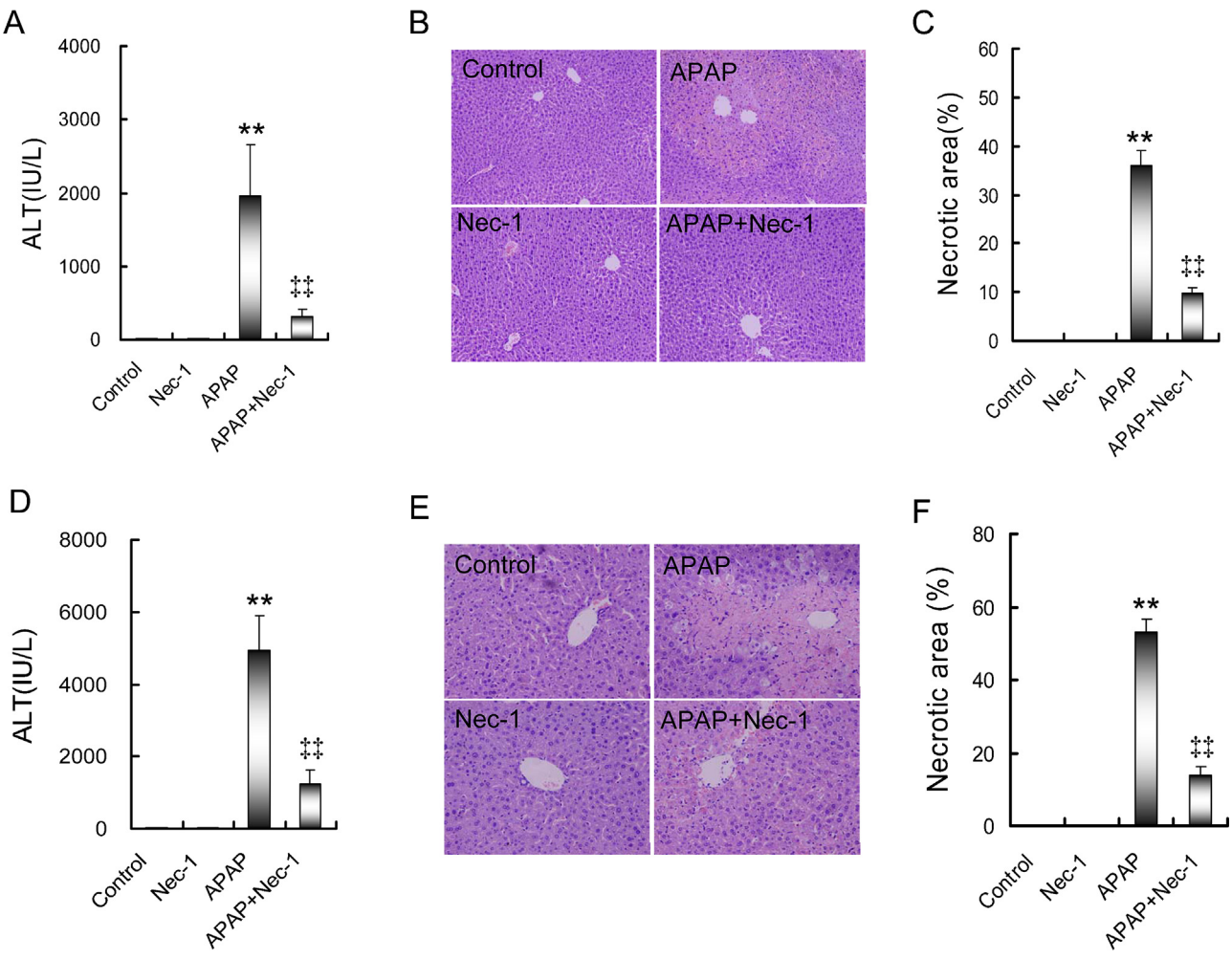

Fig. 6. Effects of post-treatment with Nec-1 on APAP-induced liver injury. Mice were i.p. injected with APAP (300 mg/kg). In APAP + Nec-1 group, mice were i.p. injected with Nec-1 (0.125 mg/mouse) 30 min after APAP. (A–C) Serum and liver samples were collected 4 h after APAP. (A) Serum ALT. (B) Representative photomicrographs of liver histology (H & E, magnification: 100×). (C) The percentage of necrotic area was analyzed. (D–F) Serum and liver samples were collected 24 h after APAP. (D) Serum ALT. (E) Representative photomicrographs of liver histology (H & E, magnification: 100×). (F) The percentage of necrotic area was analyzed. All data were expressed as means ± SEM ($n = 6$). ** $P < 0.01$ as compared with the control. ‡‡ $P < 0.01$ as compared with APAP group.

the synthesis of GSH. To examine whether Nec-1 protects against APAP-induced hepatocyte death through regulating GSH synthesis, BSO, a specific and irreversible inhibitor of γ-GCS, was used to deplete intracellular GSH. As expected, Nec-1's effect on intracellular GSH levels was completely abolished by BSO (Fig. 5B and C). Interestingly, Nec-1 could still protect against APAP-induced elevation of ALT although mice were pretreated with BSO (Fig. 5D and E). Moreover, Nec-1 significantly prevented from APAP-induced nuclear AIF translocation (Fig. 5F) and hepatocyte death (Fig. 5G and H) in mice treated with BSO.

3.8. Post-treatment with Nec-1 protects against APAP-induced hepatotoxicity

The effects of post-treatment with Nec-1 on APAP-induced acute liver injury were then analyzed. As shown in Fig. 6A and D, post-treatment with Nec-1 significantly alleviated APAP-induced increase in serum ALT. Correspondingly, post-treatment with Nec-1 significantly attenuated APAP-induced centrilobular necrosis (Fig. 6B, C, E and F).

4. Discussion

The mode of cell death caused by overdose APAP is generally considered as oncotic necrosis (Jaeschke and Bajt, 2006). A recent report demonstrates that RIP3, a critical mediator of necroptosis, plays an important role in APAP-induced acute liver failure (Ramachandran et al., 2013), suggesting that necroptosis is a mode of APAP-induced cell death. RIP1 is another mediator of necroptosis (Hitomi et al., 2008). A recent report found that Nec-1, a selective inhibitor of RIP1 (Degterev et al., 2008; Xie et al., 2013), protects against APAP-induced lethal hepatic failure (An et al., 2013). The present study showed that hepatic RIP1 was significantly upregulated as early as 1 h after APAP, which is earlier than APAP-induced upregulation of hepatic RIP3. Either pretreatment or post-treatment with Nec-1 protected against APAP-induced acute liver failure. Moreover, Nec-1 improved the survival and provented APAP-induced necroptosis. These results suggest that RIP1, an upstream molecule of RIP3, is an earlier mediator of necroptosis during APAP-induced acute liver failure.

TNF receptor 1 (TNFR1) is the most important initiator of RIP1 signaling that is involved in the process of necroptosis (Vandenabeele et al., 2010). However, an earlier report demonstrated that tnf/lt-α-deficient mice did not protect against APAP-evoked hepatotoxicity (Boess et al., 1998). Indeed, the present study found that a hepatotoxic dose of APAP did not upregulate the expression of hepatic TNF-α mRNA, whereas hepatic RIP1 was activated 1 h after APAP. Thus, TNF-α is unlikely to be a key initiator of RIP1 signaling at early stage of APAP-induced acute liver failure. In the present study, we showed that hepatic RIP1 was

significantly elevated as early as 1 h after APAP when hepatic GSH was depleted by 80%. NAC, a GSH precursor, almost completely inhibited APAP-induced elevation of hepatic RIP1 and its downstream molecule RIP3. These results suggest that excessive GSH depletion contributes, at least partially, to APAP-induced activation of hepatic RIP1 and RIP3. Indeed, NAC is the most effective antidote for APAP-induced hepatotoxicity (Polson and Lee, 2005). Several studies indicate that NAC prevents APAP-induced hepatotoxicity through scavenging reactive oxygen and peroxynitrite and by supporting the mitochondrial energy metabolism (Corcoran et al., 1985; Saito et al., 2010a,b). The present study demonstrates for the first time, to our knowledge, that NAC protects against APAP-induced acute liver failure through inhibiting hepatic RIP1 and its downstream molecule RIP3.

Increasing evidence demonstrates that the sustained activation of JNK plays a major role in APAP-induced acute liver failure (Gunawan et al., 2006). Indeed, the present study observed hepatic JNK activation in APAP-treated mice. Moreover, phosphorylated JNK in mitochondria was significantly elevated when mice were injected with a hepatotoxic dose of APAP. These results are in agreement with a recent report (Hanawa et al., 2008), in which activated JNK in cytoplasm was translocated to mitochondria in APAP-treated mice. The upstream molecule that triggers hepatic JNK activation during APAP-induced acute liver failure remains with debate. An earlier study found that RIP1 was upstream molecule of JNK in poly(ADP-ribose) polymerase-1 (PARP-1)-induced cell death (Xu et al., 2006). According to an in vitro report, inhibition of RIP1 by Nec-1, the selective inhibitor of RIP1, had no effect on APAP-induced JNK activation (Sharma et al., 2012). Recently, an in vivo study found that Nec-1 completely blocked JNK activation in response to APAP challenge (An et al., 2013). Indeed, the present study showed that APAP-evoked activation of hepatic RIP1 (maximal at 1 h after APAP) preceded hepatic JNK activation (maximal at 4 h after APAP). Moreover, Nec-1 not only repressed hepatic JNK activation, but also attenuated phosphorylated JNK translocation from the cytoplasm to the mitochondria in response to APAP challenge. These results suggest that RIP1 may play an important role in APAP-induced hepatic JNK activation.

Several studies have demonstrated that JNK activation promotes translocation of Bax, a proapoptotic protein, from the cytoplasm to the mitochondria (Kim et al., 2006; Tsuruta et al., 2004). Indeed, Bax that is translocated to the mitochondria can form pores in the outer mitochondrial membrane and promote the early release of AIF from the mitochondria to the nuclei (Bajt et al., 2008). According to a recent report, AIF, which is translocated to the nuclei from the mitochondria, is responsible for the initial DNA fragmentation and necrotic cell death during APAP-induced acute liver failure (Saito et al., 2010a,b). The present study found that Nec-1, the specific inhibitor of RIP1, obviously inhibited APAP-induced translocation of Bax from the cytoplasm to the mitochondria. Moreover, Nec-1 almost completely inhibited APAP-evoked translocation of AIF from the mitochondria to the nuclei. These results suggest that mitochondrial Bax translocation and subsequent nuclear AIF translocation are downstream events following RIP1-mediated JNK activation in the process of APAP-induced necroptosis.

Although Nec-1 is not an antioxidant, Nec-1 can attenuate glutamate-induced GSH depletion and ROS production (Xu et al., 2007). According to a recent report, a single dose of Nec-1 significantly alleviated oxidative damage to proteins during the first 24 h after neonatal hypoxia–ischemia (Northington et al., 2011). The present study found that pretreatment with Nec-1 significantly attenuated hepatic GSH depletion 4 h after APAP. Moreover, Nec-1 significantly alleviated APAP-induced hepatic protein nitrification. To examine whether Nec-1 protects against APAP-induced necroptosis through regulating hepatic GSH synthesis, BSO, a specific and irreversible inhibitor of γ-GCS, was used to deplete intracellular GSH. Unexpectedly, the protective effect of Nec-1 on APAP-induced necroptosis was still observed although cellular GSH was depleted by BSO. The present study also investigated whether Nec-1 by itself could alter APAP metabolism. As expected, hepatic GSH was significantly decreased 30 min after APAP. Of interest, pretreatment with Nec-1 did not affect the level of hepatic GSH at 30 min after APAP. In addition, Nec-1 had no effect on the expression of hepatic CYP2E1, a key enzyme for APAP metabolism. These results suggest that Nec-1-mediated protection against APAP-induced necroptosis is mainly attributed to its inhibition of RIP1.

In summary, the present study demonstrated that hepatic RIP1 activation is an early event during APAP-induced acute liver failure. Either pretreatment or post-treatment with Nec-1, a selective inhibitor of RIP1, protects against APAP-induced acute liver failure. Moreover, Nec-1 represses APAP-induced hepatic JNK activation and Bax translocation from the cytoplasm to the mitochondria. The present study demonstrated that Nec-1 protects against AIF-mediated necroptosis during APAP-induced acute liver failure. Thus, Nec-1 is an effective antidote for APAP-induced acute liver failure.

Transparency document

The authors declare that there are no conflicts of interest.

Acknowledgments

This project was supported by National Natural Science Foundation of China (81373495, 30371667, 30572223, 30973544, 81001480) and Natural Science Foundation of Anhui province (090413142, 1308085MH120), Key Project of the Department of Education of Anhui in China (KJ2011A159) and the University Excellence Young Talent Fund of Educational Commission of Anhui Province (2011SQRL058).

References

Anderson, M.E., 1985. Determination of glutathione and glutathione disulfide in biological samples. Methods Enzymol. 113, 548–555.

An, J., Mehrhof, F., Harms, C., Lättig-Tünnemann, G., Lee, S.L., Endres, M., Li, M., Sellge, G., Mandić, A.D., Trautwein, C., Donath, S., 2013. ARC is a novel therapeutic approach against acetaminophen-induced hepatocellular necrosis. J. Hepatol. 58, 297–305.

Bajt, M.L., Cover, C., Lemasters, J.J., Jaeschke, H., 2006. Nuclear translocation of endonuclease G and apoptosis-inducing factor during acetaminophen-induced liver cell injury. Toxicol. Sci. 94, 217–225.

Bajt, M.L., Farhood, A., Lemasters, J.J., Jaeschke, H., 2008. Mitochondrial bax translocation accelerates DNA fragmentation and cell necrosis in a murine model of acetaminophen hepatotoxicity. J. Pharmacol. Exp. Ther. 324, 8–14.

Bajt, M.L., Ramachandran, A., Yan, H.M., Lebofsky, M., Farhood, A., Lemasters, J.J., Jaeschke, H., 2011. Apoptosis-inducing factor modulates mitochondrial oxidant stress in acetaminophen hepatotoxicity. Toxicol. Sci. 122, 598–605.

Boess, F., Bopst, M., Althaus, R., Polsky, S., Cohen, S.D., Eugster, H.P., Boelsterli, U.A., 1998. Acetaminophen hepatotoxicity in tumor necrosis factor/lymphotoxin-alpha gene knockout mice. Hepatology 27, 1021–1029.

Carmona-Gutierrez, D., Eisenberg, T., Buttner, S., Meisinger, C., Kroemer, G., Madeo, F., 2010. Apoptosis in yeast: triggers, pathways, subroutines. Cell Death Differ. 17, 763–773.

Corcoran, G.B., Racz, W.J., Smith, C.V., Mitchell, J.R., 1985. Effects of *N*-acetylcysteine on acetaminophen covalent binding and hepatic necrosis in mice. J Pharmacol. Exp. Ther. 232, 864–872.

Degterev, A., Hitomi, J., Germscheid, M., Ch'en, I.L., Korkina, O., Teng, X., Abbott, D., Cuny, G.D., Yuan, C., Wagner, G., Hedrick, S.M., Gerber, S.A., Lugovskoy, A., Yuan, J., 2008. Identification of RIP1 kinase as a specific cellular target of necrostatins. Nat. Chem. Biol. 4, 313–321.

Duprez, L., Takahashi, N., Van Hauwermeiren, F., Vandendriessche, B., Goossens, V., Vanden Berghe, T., Declercq, W., Libert, C., Cauwels, A., Vandenabeele, P., 2011. RIP kinase-dependent necrosis drives lethal systemic inflammatory response syndrome. Immunity 35, 908–918.

Ferlini, A., Rimessi, P., 2012. Exon skipping quantification by real-time PCR. Methods Mol. Biol. 867, 189–199.

Galluzzi, L., Maiuri, M.C., Vitale, I., Zischka, H., Castedo, M., Zitvogel, L., Kroemer, G., 2007. Cell death modalities: classification and pathophysiological implications. Cell Death Differ. 14, 1237–1243.

Galluzzi, L., Vitale, I., Abrams, J.M., Alnemri, E.S., Baehrecke, E.H., Blagosklonny, M.V., Dawson, T.M., Dawson, V.L., El-Deiry, W.S., Fulda, S., Gottlieb, E., Green, D.R., Hengartner, M.O., Kepp, O., Knight, R.A., Kumar, S., Lipton, S.A., Lu, X., Madeo, F., Malorni, W., Mehlen, P., Nunez, G., Peter, M.E., Piacentini, M., Rubinsztein, D.C., Shi, Y., Simon, H.U., Vandenabeele, P., White, E., Yuan, J., Zhivotovsky, B., Melino, G., Kroemer, G., 2012. Molecular definitions of cell death subroutines: recommendations of the Nomenclature Committee on Cell Death 2012. Cell Death Differ. 19, 107–120.

Ghosh, J., Das, J., Manna, P., Sil, P.C., 2010. Arjunolic acid, a triterpenoid saponin, prevents acetaminophen (APAP)-induced liver and hepatocyte injury via the inhibition of APAP bioactivation and JNK-mediated mitochondrial protection. Free Radical Biol. Med. 48, 535–553.

Gunawan, B.K., Liu, Z.X., Han, D., Hanawa, N., Gaarde, W.A., Kaplowitz, N., 2006. c-Jun N-terminal kinase plays a major role in murine acetaminophen hepatotoxicity. Gastroenterology 131, 165–178.

Hanawa, N., Shinohara, M., Saberi, B., Gaarde, W.A., Han, D., Kaplowitz, N., 2008. Role of JNK translocation to mitochondria leading to inhibition of mitochondria bioenergetics in acetaminophen-induced liver injury. J. Biol. Chem. 283, 13565–13577.

Hitomi, J., Christofferson, D.E., Ng, A., Yao, J., Degterev, A., Xavier, R.J., Yuan, J., 2008. Identification of a molecular signaling network that regulates a cellular necrotic cell death pathway. Cell 135, 1311–1323.

Hoebeeck, J., Speleman, F., Vandesompele, J., 2007. Real-time quantitative PCR as an alternative to southern blot or fluorescence in situ hybridization for detection of gene copy number changes. Methods Mol. Biol. 353, 205–226.

Jaeschke, H., Bajt, M.L., 2006. Intracellular signaling mechanisms of acetaminophen-induced liver cell death. Toxicol. Sci. 89, 31–41.

Kaiser, W.J., Upton, J.W., Long, A.B., Livingston-Rosanoff, D., Daley-Bauer, L.P., Hakem, R., Caspary, T., Mocarski, E.S., 2011. RIP3 mediates the embryonic lethality of caspase-8-deficient mice. Nature 471, 368–372.

Kim, B.J., Ryu, S.W., Song, B.J., 2006. JNK- and p38 kinase-mediated phosphorylation of Bax leads to its activation and mitochondrial translocation and to apoptosis of human hepatoma HepG2 cells. J. Biol. Chem. 281, 21256–21265.

Kumar, S., 2007. Caspase function in programmed cell death. Cell Death Differ. 14, 32–43.

Latchoumycandane, C., Goh, C.W., Ong, M.M., Boelsterli, U.A., 2007. Mitochondrial protection by the JNK inhibitor leflunomide rescues mice from acetaminophen-induced liver injury. Hepatology 45, 412–421.

Northington, F.J., Chavez-Valdez, R., Graham, E.M., Razdan, S., Gauda, E.B., Martin, L.J., 2011. Necrostatin decreases oxidative damage, inflammation, and injury after neonatal HI. J. Cereb. Blood Flow Metab. 31, 178–189.

Orrenius, S., Nicotera, P., Zhivotovsky, B., 2011. Cell death mechanisms and their implications in toxicology. Toxicol. Sci. 119, 3–19.

Osborn, S.L., Diehl, G., Han, S.J., Xue, L., Kurd, N., Hsieh, K., Cado, D., Robey, E.A., Winoto, A., 2010. Fas-associated death domain (FADD) is a negative regulator of T-cell receptor-mediated necroptosis. PNAS 107, 13034–13039.

Polson, J., Lee, W.M., 2005. AASLD position paper: the management of acute liver failure. Hepatology 41, 1179–1197.

Ramachandran, A., Lebofsky, M., Weinman, S.A., Jaeschke, H., 2011. The impact of partial manganese superoxide dismutase (SOD2)-deficiency on mitochondrial oxidant stress, DNA fragmentation and liver injury during acetaminophen hepatotoxicity. Toxicol. Appl. Pharmacol. 251, 226–233.

Ramachandran, A., McGill, M.R., Xie, Y., Ni, H.M., Ding, W.X., Jaeschke, H., 2013. The receptor interacting protein kinase 3 is a critical early mediator of acetaminophen-induced hepatocyte necrosis in mice. Hepatology 58, 2099–2108.

Saito, C., Lemasters, J.J., Jaeschke, H., 2010a. c-Jun N-terminal kinase modulates oxidant stress and peroxynitrite formation independent of inducible nitric oxide synthase in acetaminophen hepatotoxicity. Toxicol. Appl. Pharmacol. 246, 8–17.

Saito, C., Zwingmann, C., Jaeschke, H., 2010b. Novel mechanisms of protection against acetaminophen hepatotoxicity in mice by glutathione and *N*-acetylcysteine. Hepatology 51, 246–254.

Sharma, M., Gadang, V., Jaeschke, A., 2012. Critical role for mixed-lineage kinase 3 in acetaminophen-induced hepatotoxicity. Mol. Pharmacol. 82, 1001–1007.

Shen, H.M., Codogno, P., 2011. Autophagic cell death: Loch Ness monster or endangered species? Autophagy 7, 457–465.

Trichonas, G., Murakami, Y., Thanos, A., Morizane, Y., Kayama, M., Debouck, C.M., Hisatomi, T., Miller, J.W., Vavvas, D.G., 2010. Receptor interacting protein kinases mediate retinal detachment-induced photoreceptor necrosis and compensate for inhibition of apoptosis. PNAS 107, 21695–21700.

Tsuruta, F., Sunayama, J., Mori, Y., Hattori, S., Shimizu, S., Tsujimoto, Y., Yoshioka, K., Masuyama, N., Gotoh, Y., 2004. JNK promotes Bax translocation to mitochondria through phosphorylation of 14-3-3 proteins. EMBO J. 23, 1889–1899.

Vandenabeele, P., Galluzzi, L., Vanden Berghe, T., Kroemer, G., 2010. Molecular mechanisms of necroptosis: an ordered cellular explosion. Nat. Rev. Mol. Cell Biol. 11, 700–714.

Vanlangenakker, N., Vanden Berghe, T., Vandenabeele, P., 2012. Many stimuli pull the necrotic trigger, an overview. Cell Death Differ. 19, 75–86.

Xie, T., Peng, W., Liu, Y., Yan, C., Maki, J., Degterev, A., Yuan, J., Shi, Y., 2013. Structural basis of RIP1 inhibition by necrostatins. Structure 21, 493–499.

Xu, X., Chua, C.C., Kong, J., Kostrzewa, R.M., Kumaraguru, U., Hamdy, R.C., Chua, B.H., 2007. Necrostatin-1 protects against glutamate-induced glutathione depletion and caspase-independent cell death in HT-22 cells. J. Neurochem. 103, 2004–2014.

Xu, Y., Huang, S., Liu, Z.G., Han, J., 2006. Poly(ADP-ribose) polymerase-1 signaling to mitochondria in necrotic cell death requires RIP1/TRAF2-mediated JNK1 activation. J. Biol. Chem. 281, 8788–8795.

Zaher, H., Buters, J.T., Ward, J.M., Bruno, M.K., Lucas, A.M., Stern, S.T., Cohen, S.D., Gonzalez, F.J., 1998. Protection against acetaminophen toxicity in CYP1A2 and CYP2E1 double-null mice. Toxicol. Appl. Pharmacol. 152, 193–199.